^{18}F-FLT PET/CT for Early Response Monitoring and Dose Escalation in Oropharyngeal Tumors

Esther G.C. Troost[1], Johan Bussink[1], Aswin L. Hoffmann[1], Otto C. Boerman[2], Wim J.G. Oyen[2], and Johannes H.A.M. Kaanders[1]

[1]Department of Radiation Oncology, Institute of Oncology, Radboud University Nijmegen Medical Centre, Nijmegen, The Netherlands; and [2]Department of Nuclear Medicine, Institute of Oncology, Radboud University Nijmegen Medical Centre, Nijmegen, The Netherlands

Accelerated tumor cell proliferation is an important mechanism adversely affecting therapeutic outcome in head and neck cancer. 3′-deoxy-3′-^{18}F-fluorothymidine (^{18}F-FLT) is a PET tracer to noninvasively image tumor cell proliferation. The aims of this study were to monitor early tumor response based on repetitive ^{18}F-FLT PET/CT scans and to identify subvolumes with high proliferative activity eligible for dose escalation. **Methods:** Ten patients with oropharyngeal tumors underwent an ^{18}F-FLT PET/CT scan before and twice during radiotherapy. The primary tumor and metastatic lymph nodes (gross tumor volume, or GTV) were delineated on CT (GTV_{CT}) and after segmentation of the PET signal using the 50% isocontour of the maximum signal intensity or an adaptive threshold based on the signal-to-background ratio (GTV_{SBR}). GTVs were calculated, and similarity between GTV_{CT} and GTV_{SBR} was assessed. Within GTV_{SBR}, the maximum and mean standardized uptake value (SUV_{max} and SUV_{mean}, respectively) was calculated. Within GTV_{CT}, tumor subvolumes with high proliferative activity based on the 80% isocontour ($GTV_{80\%}$) were identified for radiotherapy planning with dose escalation. **Results:** The GTV_{CT} decreased significantly in the fourth week but not in the initial phase of treatment. SUV_{max} and SUV_{mean} decreased significantly as early as 1 wk after therapy initiation and even further before the fourth week of treatment. For the primary tumor, the average ($\pm$SD) SUV_{mean} of the GTV_{SBR} was 4.7 $\pm$ 1.6, 2.0 $\pm$ 0.9, and 1.3 $\pm$ 0.2 for the consecutive scans ($P < 0.0001$). The similarity between GTV_{CT} and GTV_{SBR} decreased during treatment, indicating an enlargement of GTV_{SBR} outside GTV_{CT} caused by the increasing difficulty of segmenting tracer uptake in the tumor from the background and by proliferative activity in the nearby tonsillar tissue. $GTV_{80\%}$ was successfully identified in all primary tumors and metastatic lymph nodes, and dose escalation based on the $GTV_{80\%}$ was demonstrated to be technically feasible. **Conclusion:** ^{18}F-FLT is a promising PET tracer for imaging tumor cell proliferation in head and neck carcinomas. Signal changes in ^{18}F-FLT PET precede volumetric tumor response and are therefore suitable for early response assessment. Definition of tumor subvolumes with high proliferative activity and dose escalation to these regions are technically feasible.

Key Words: ^{18}F-fluorothymidine-PET; head and neck cancer; early response monitoring; adaptive radiotherapy; dose escalation

J Nucl Med 2010; 51:866–874
DOI: 10.2967/jnumed.109.069310

Radiotherapy with or without concomitant chemotherapy is the therapy of choice for advanced-stage primary squamous cell carcinomas of the oropharynx (*1*). For radiation therapy planning, a single CT scan in treatment position is acquired before the initiation of treatment. Traditionally, a homogeneous dose distribution is prescribed to the gross tumor volume (GTV) defined on CT, with a margin for subclinical growth and setup inaccuracy. In the last decade, intensity-modulated radiation therapy (IMRT) revolutionized the field of radiotherapy. IMRT is based on the use of photon beams with optimized nonuniform fluence profiles. With this technique, the simultaneous delivery of different dose prescriptions to various target subsites became feasible. Certain areas within the GTV can be boosted to higher doses, and steep dose gradients allow reduction of the dose delivered to radiation-sensitive tissues adjacent to the tumor (*2,3*). However, precise knowledge about the tumor location and extension is compulsory, and tumor areas requiring higher radiation doses must be identified.

Functional imaging can complement anatomic imaging modalities such as CT and MRI and provide biologic tumor information relevant to radiotherapy dose planning. Initial studies with PET using ^{18}F-FDG showed that the volume irradiated to high-dose levels can be reduced, thus sparing normal structures and promoting dose escalation (*4–9*). ^{18}F-FDG uptake reflects metabolic activity, and false-positive readings are caused by tracer uptake in inflammatory

Received Aug. 25, 2009; revision accepted Nov. 23, 2009.
For correspondence or reprints contact: Esther G.C. Troost, Department of Radiation Oncology, Institute of Oncology, Radboud University Nijmegen Medical Centre, P.O. Box 9101, 6500 HB Nijmegen, The Netherlands.
E-mail: e.troost@rther.umcn.nl

tissue. Other PET tracers can provide more specific biologic information, in particular on radiotherapy resistance mechanisms.

Accelerated repopulation of tumor cells during the course of radiotherapy is a frequently observed phenomenon in squamous cell carcinomas of the head and neck that adversely affects treatment outcome (*10,11*). 3′-deoxy-3′-^{18}F-fluorothymidine (^{18}F-FLT) uptake is enhanced during DNA synthesis, and ^{18}F-FLT PET therefore provides a noninvasive way to image tumor cell proliferation (*12–15*). Potential applications of ^{18}F-FLT PET in radiation oncology include patient selection for treatment modification based on the proliferative state of the tumor, identification of tumor subvolumes with a high density of actively proliferating cells amenable to boosting, and early monitoring of response to treatment.

In this study, patients with oropharyngeal tumors underwent 3 consecutive ^{18}F-FLT PET scans: once before and twice during the course of radiotherapy. The aims of this study were to monitor early tumor response based on ^{18}F-FLT PET/CT volume and ^{18}F-FLT PET signal changes, to assess the heterogeneity of intratumoral ^{18}F-FLT distribution and identify subvolumes with a high density of proliferating cells, and to determine the technical feasibility of adaptive radiation therapy based on ^{18}F-FLT PET/CT.

MATERIALS AND METHODS

Patients

From March 2007 until September 2008, 10 patients with newly diagnosed primary oropharyngeal carcinomas eligible for radiotherapy with or without concomitant chemotherapy were included in this study after giving written informed consent. The Institutional Review Board of the Radboud University Nijmegen Medical Centre approved the study.

Treatment

The patients were treated with IMRT with a simultaneous integrated boost technique, delivering a dose of 68 Gy in fractions of 2 Gy to the primary tumor and metastatic cervical lymph nodes and 50.3 Gy in fractions of 1.48 Gy to the electively treated neck nodes. An accelerated fractionation schedule was used with an overall treatment time of 5.5 wk, delivering 2 fractions per day during the last 1.5 wk of the treatment. In accordance with the guidelines of the institution, 2 patients with bulky primary tumors were concomitantly treated with cisplatinum, 40 mg/m^2, administered intravenously once weekly.

^{18}F-FLT Synthesis

^{18}F-FLT was obtained from the Department of Nuclear Medicine and PET Research, VU University Medical Centre, Amsterdam, The Netherlands. The synthesis was performed according to the method of Machulla et al. (*16*). Briefly, ^{18}F-FLT was produced by ^{18}F-fluorination of the 4,4′-dimethoxytrityl–protected anhydrothymidine, followed by a deprotection step. The product was purified by reversed-phase high-performance liquid chromatography, made isotonic, and passed through a 0.22-μm filter. ^{18}F-FLT was routinely produced with a non–decay-corrected radiochemical yield of 5%−10%, a radiochemical purity of more than 97%, and a specific activity of more than 10,000 GBq/mmol.

^{18}F-FLT PET/CT Acquisition

Before and in the second and fourth weeks of radiotherapy, integrated ^{18}F-FLT PET and CT images were acquired on a hybrid PET/CT scanner (Biograph Duo; Siemens/CTI). All scans were performed with the patient supine and immobilized with an individual head support and a rigid customized mask covering the head and neck area to increase positioning accuracy and to reduce movement artifacts during image acquisition. Emission images of the head and neck area were recorded 60 min after the intravenous injection of approximately 250 MBq of ^{18}F-FLT, with 7 min per bed position in 3-dimensional mode. PET images were reconstructed using the ordered-subsets expectation maximization iterative algorithm with parameters optimized for the head and neck area (i.e., 4 iterations, 16 subsets, and a 5-mm 3-dimensional gaussian filter (*17*)) and correction for photon attenuation. In addition, CT images were acquired for anatomic correlation and attenuation correction using 80 mAs, 130 kV, a 3-mm slice width, and intravenous contrast material in the venous phase (Optiray; Mallinckrodt Inc.).

^{18}F-FLT PET Analysis

After reconstruction, standardized uptake value (SUV) PET images were created with software developed in-house correcting for injected dose, decay of the tracer, and patient body weight. Subsequently, these SUV PET images were resliced using the CT format as a reference. SUV PET and CT images were imported into Pinnacle^3 (version 8.0d; Philips Radiation Oncology Systems), the radiotherapy planning system routinely used at our department. With this software, the consecutive CT and PET scans were registered to the first CT scan using cross correlation. Two investigators delineated the GTV of the primary tumor and the metastatic lymph nodes on all registered CT scans (GTV_{CT}).

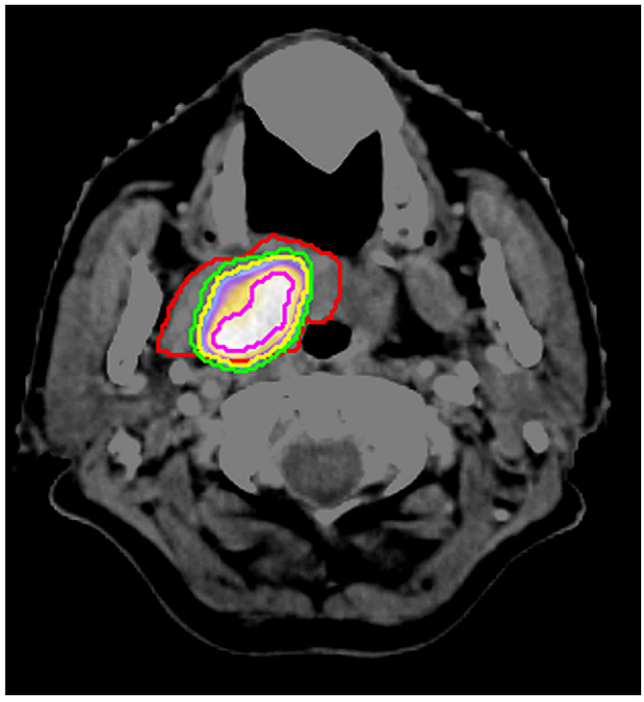

FIGURE 1. ^{18}F-FLT PET/CT image of T3N0M0 oropharyngeal tumor before radiation therapy. Shown are GTV_{CT} (red), GTV_{SBR} (green), and $GTV_{50\%}$. $GTV_{80\%}$ is highlighted in pink.

Self-written scripts in Pinnacle[3] were used for the segmentation of the primary tumor and the metastatic lymph nodes from the PET images and for the calculation of the mean and maximum SUV (SUV_{mean} and SUV_{max}) within these volumes.

PET Segmentation

Primary Tumor and Metastatic Lymph Nodes. Two previously described methods for segmentation of the primary tumor and the metastatic lymph nodes in the PET images were applied (*7,18*). First, the 50% isocontour was based on a fixed percentage of the maximum signal intensity in the primary tumor (GTV50%). Second, an adaptive threshold delineation based on the signal-to-background ratio was performed (GTV_{SBR}) (Fig. 1) (*18*). For this means, the SUV_{max} was defined as mean uptake of the hottest voxel in the tumor or metastatic lymph node and its 8 surrounding voxels in 1 transversal slice. Mean background uptake was calculated from a manually defined region of interest in the left neck musculature (~10 cm^3) at a sufficient distance from the vertebrae, the primary tumor, and lymph node metastases.

Subvolumes with High Proliferative Activity. Based on the ^{18}F-FLT PET signal, tumor subvolumes with a high density of proliferating tumor cells within the GTV_{CT} of the primary tumor and metastatic lymph nodes were defined. An arbitrary, fixed threshold of the SUV_{max} was defined that fulfilled the requirement of delineating a tumor subvolume in at least the first and second ^{18}F-FLT PET scans. This requirement was best met using the 80% isocontour ($GTV_{80\%}$). The absolute $GTV_{80\%}$ and the fraction of the $GTV_{80\%}$ relative to the GTV_{CT} were calculated. The $GTV_{80\%}$ from the third scan was not further analyzed, because of a low ^{18}F-FLT uptake in the tumor and thus a relatively low SUV_{max} within the GTV_{CT}. This led to unsuccessful segmentation of PET subvolumes, which were mostly larger than the GTV_{CT} and often encompassed the entire tonsillar region.

Volumetric and Spatial Similarity

The absolute volumetric similarity of GTV_{CT} and GTV_{SBR} was assessed at all 3 time points. For this analysis, only GTV_{SBR} was used. As it does not adjust for background activity, segmentation of the tumor by GTV50% became increasingly difficult with lower ^{18}F-FLT-uptake in the second and third scans.

As measures of volumetric similarity, we calculated the part of the GTV_{CT} that was not covered by the GTV_{SBR} and vice versa: the GTV_{SBR} not enclosed by the GTV_{CT}. As a measure reflecting differences in location more strongly than differences in size, the dice similarity coefficient (DSC) was additionally calculated as twice the overlap volume divided by the sum of both volumes: $DSC = 2 \times (GTV_{CT} \cap GTV_{SBR})/(GTV_{CT} + GTV_{SBR})$ (*19*). It is generally accepted that a value of DSC greater than 0.7 represents excellent agreement (*20*). The same calculations were applied to $GTV_{80\%}$ delineated on the first and second ^{18}F-FLT PET scans, $GTV_{80\%1}$ and $GTV_{80\%2}$.

Statistical Analysis

Statistical analyses were performed using GraphPad Prism, version 4.0c (GraphPad Software, Inc.), for Macintosh (Apple, Inc.). Gaussian distribution was tested using the Kolmogorov–Smirnov test. The change in CT volumes was assessed applying repeated-measures ANOVA and the 2-tailed paired *t* test, and the change in PET volumes was assessed by applying the Friedman test and Wilcoxon signed-rank test. The alteration in PET signal intensity was assessed using the 2-tailed paired *t* test. The volumetric similarity of the GTVs delineated on CT and PET was analyzed using the Friedman test and Wilcoxon signed-rank test. The repeated-measures ANOVA and 2-tailed paired *t* test were applied to the DSC. The volumetric change in $GTV_{80\%}$ was assessed using the Wilcoxon signed-rank test. A *P* value of 0.05 or less was regarded as statistically significant.

RESULTS

Patient and Tumor Characteristics

The patient and tumor characteristics are summarized in Table 1. Eight patients were treated with radiotherapy alone, and 2 patients with the addition of concomitant chemotherapy. The first ^{18}F-FLT PET scan was acquired before the start of therapy (median, 5 d; range, 0–9 d). The second and third scans were acquired in the second and fourth weeks, respectively, of treatment (Table 1). All primary tumors and lymph node metastases were visualized and subject to further assessment.

Early Response Monitoring

Reduction of Tumor Volume. The mean GTV_{CT} decreased significantly between the second and third CT scans but not in the initial phase of treatment: mean GTV_{CT} on subsequent scans was 12.7 ± 9.5, 11.1 ± 8.8, and 5.0 ± 4.7

TABLE 1. Patient Characteristics

Patient no.	Site	Sex	Age (y)	Clinical stage	Treatment	Cumulative dose (Gy) delivered at... PET2	PET3
1	Tonsil	F	67	T3N0M0	Radiotherapy + chemotherapy	16	36
2	Soft palate	M	66	T2N1M0	Radiotherapy + chemotherapy	16	36
3	Base of tongue/tonsil	M	60	T2N0M0	Radiotherapy	12	36
4	Tonsil	M	53	T2N2bM0	Radiotherapy	16	36
5	Base of tongue/tonsil	M	69	T2N0M0	Radiotherapy	12	32
6	Tonsil	F	53	T3N0M0	Radiotherapy	24	36
7	Tonsil/hypopharynx	M	64	T2N1M0	Radiotherapy	16	36
8	Tonsil	M	55	T2N2bM0	Radiotherapy	20	36
9	Tonsil	M	70	T2N0M0	Radiotherapy	10	30
10	Tonsil	M	52	T1N2bM0	Radiotherapy	12	36

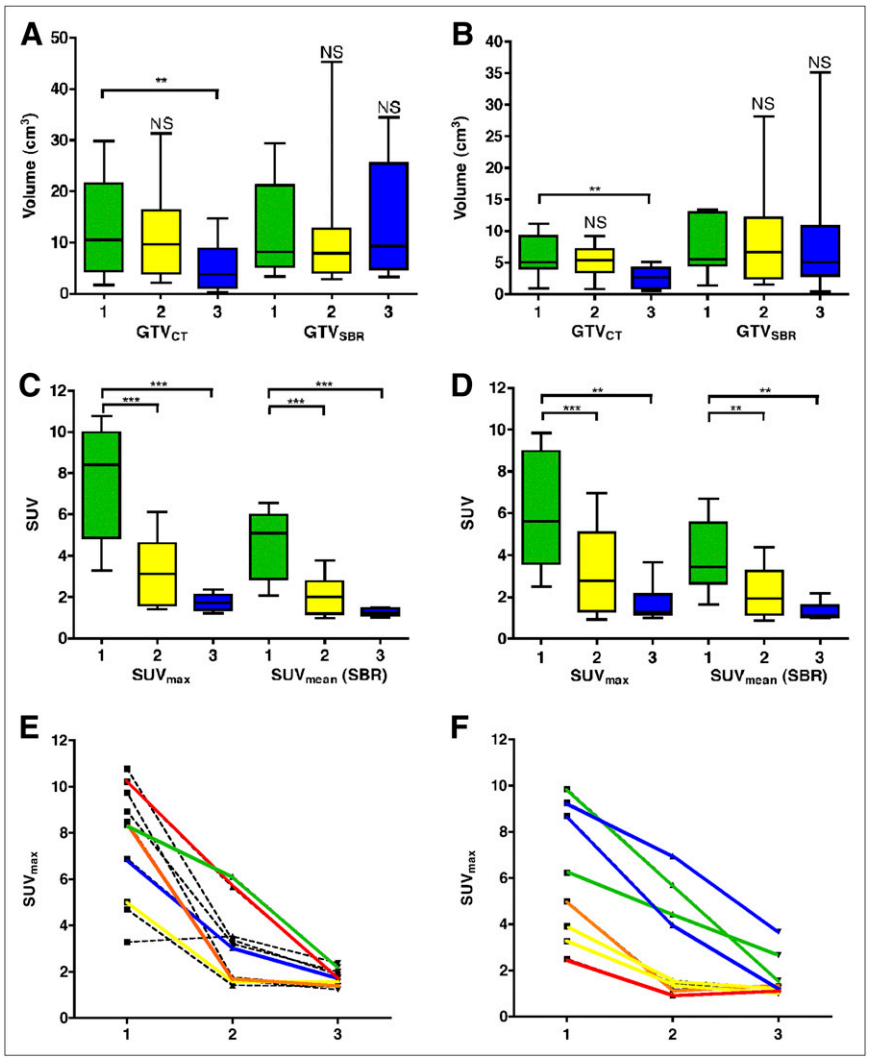

FIGURE 2. (A and B) In cubic centimeters, GTV_{CT} and GTV_{SBR} for primary tumor (A) and metastatic lymph nodes (B). (C and D) SUV_{max} and SUV_{mean} analyzed using SBR method for primary tumor (C) and metastatic lymph nodes (D). Volumes and SUVs for first (green), second (yellow), and third (blue) scans are shown. (E and F) Alteration in SUV_{max} on individual-patient basis for all primary tumors (E) and metastatic lymph nodes (F). Each patient with cervical lymph node metastases is highlighted by an identical color code. $^{*}P < 0.01$. $^{**}P < 0.001$. $^{***}P < 0.0001$. NS = not significant.

cm^3 (Fig. 2A). Although the overall ^{18}F-FLT signal intensity decreased significantly after the start of treatment, the segmented PET volume remained almost unchanged when the SBR method was used (mean GTV_{SBR} of 11.8 ± 8.9, 11.3 ± 12.4, and 14.1 ± 10.8 cm^3 [Fig. 2A]) and even increased when the 50% threshold of the maximum signal intensity was applied (mean GTV50% of 18.0 ± 31.5, 18.6 ± 21.8, and 40.9 ± 61.1). For the 2 patients treated with concomitant radiotherapy and chemotherapy, the decrease in ^{18}F-FLT PET signal was similar to that of the patients treated with radiotherapy alone.

For GTV delineation of the lymph nodes, the trends were similar to those for the primary tumors, that is, a decrease in GTV_{CT} by the end of the treatment and no significant change in GTV_{SBR} (Fig. 2B). Because the 50% method resulted in unsatisfactory results in the primary tumors, it was not further applied to the metastatic lymph nodes.

Decrease of SUV. In the primary tumors, the SUV_{max} of the second ^{18}F-FLT PET scan was already significantly decreased relative to the first scan, and the SUV_{max} decreased even further in the third (7.6 ± 2.6, 3.1 ± 1.7, and 1.7 ± 0.4; Fig. 2C). The same was observed for SUV_{mean} within GTV_{SBR} (4.7 ± 1.6, 2.0 ± 0.9, and 1.3 ± 0.2; Fig. 2C). However, on an individual-patient basis, different response patterns became apparent (Fig. 2E). On average, the relative decrease in SUV_{max} was 55% between the first and second scans and 34% between the second and third scans.

In the lymph node metastases, similar patterns were observed for SUV_{max} and SUV_{mean} (Fig. 2D). The relative decrease in SUV_{max} was 44% between the first and second scans and 47% between the second and third scans, again with individual differences (Fig. 2F).

Similarity of CT and ^{18}F-FLT PET Volume Before and During Treatment

To determine the feasibility of adaptive radiotherapy based on repetitive ^{18}F-FLT PET/CT, we assessed the absolute volumetric similarity and DSC of GTV_{CT} and GTV_{SBR} at all time points. There was a significant decrease in the absolute GTV_{CT} volume not covered by GTV_{SBR} at the third time point (Fig. 3A), indicating an almost complete coverage

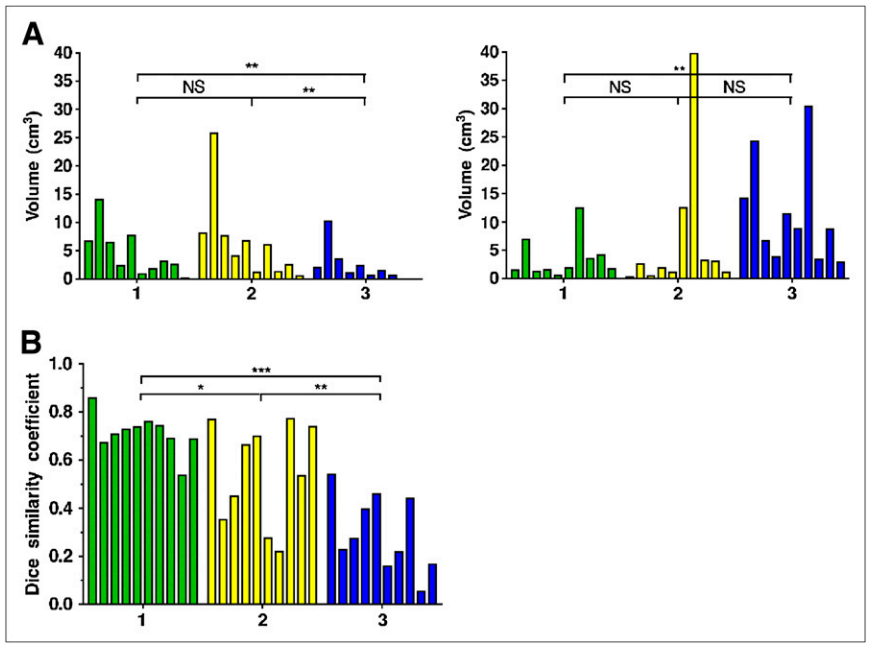

FIGURE 3. (A) GTV_{CT} volume (in cm^3) not covered by GTV_{SBR} (left graph) and GTV_{SBR} not covered by GTV_{CT} (right graph) for first (green), second (yellow), and third (blue) time points. (B) DSC calculated for CT- and ^{18}F-FLT PET–derived volumes at the 3 time points. $*P < 0.01$. $**P < 0.001$. $***P < 0.0001$. NS = not significant.

of the GTV_{CT} by the GTV_{SBR}. On the other hand, there was a significant increase in the GTV_{SBR} volume not enclosed by GTV_{CT}, indicating a large GTV_{SBR} outside the GTV_{CT} that even increased over time (Fig. 3A). This decrease in volumetric and especially in spatial concordance was reflected by a significant decline of the DSC at the second and third PET scans (Fig. 3B). The mean DSC was 0.71 ± 0.08, 0.55 ± 0.21, and 0.29 ± 0.16 on the consecutive scans. This decrease in concordance was partly caused by increasing tracer uptake in the tonsillar region, especially in the fourth week of treatment, and partly by low tracer uptake in the primary tumor, hampering the adaptive threshold method.

Delineation of Subvolume with High Density of Proliferating Cells Using ^{18}F-FLT PET

For all primary tumors, a $GTV_{80\%}$ within the GTV_{CT} could be identified on the first and second ^{18}F-FLT PET/CT scans (Supplemental Fig. 1). In the third scan, this identification was hampered by a relatively low ^{18}F-FLT uptake in the tumor relative to the background, leading to unsuccessful segmentation and subsequently to PET subvolumes larger than the GTV_{CT}, often encompassing the entire tonsillar region. The average $GTV_{80\%}$ decreased slightly between the first and second scans (1.52 ± 1.76 and 0.93 ± 0.94 cm^3, respectively). Compared with the GTV_{CT}, the $GTV_{80\%}$ was relatively small and the fraction $GTV_{80\%}/GTV_{CT}$ overall did not change during treatment (before treatment, 0.12 ± 0.07; second week of treatment, 0.12 ± 0.14). On an individual-patient basis, however, remarkable changes occurred in some cases, such as in patients 1, 7, and 8 (Supplemental Fig. 1). Between the first and second scans, the $GTV_{80\%}$ decreased and was displaced (patients 1 and 7) or substantially increased (patient 8). To assess these changes in size and location of the $GTV_{80\%}$, we calculated the absolute volumetric similarity and DSC of $GTV_{80\%1}$ and $GTV_{80\%2}$. The average volume of the $GTV_{80\%1}$ not covered by $GTV_{80\%2}$ was 1.12 ± 1.67 cm^3 and the average volume of the $GTV_{80\%2}$ not encompassed by $GTV_{80\%1}$ was 0.56 ± 0.86 cm^3. The mean overall DSC was 0.47 ± 0.25, indicating a moderate spatial similarity between the first and second tumor subvolumes. However, there were large interindividual differences, reflected by a range in DSC of 0.03–0.86.

For all lymph node metastases, a subvolume with a high density of proliferating cells could also be identified. The mean absolute overall volume did not significantly change between the first and second scans (1.20 ± 1.13 and 1.21 ± 1.25 cm^3, respectively), nor did the mean fraction of $GTV_{80\%}$, compared with the GTV_{CT} (before treatment, 0.17 ± 0.08; second week of treatment, 0.19 ± 0.14).

Generation of IMRT Plan with Boost to ^{18}F-FLT PET–Delineated Subvolumes

As a proof of principle, an adaptive IMRT treatment plan with simultaneous integrated boost and an accelerated schedule was generated for a patient with a T3N0M0 oropharyngeal tumor. This plan was based on the CT scan acquired before treatment, taking into account changes in proliferative activity occurring during treatment (Fig. 4). With this technique, the neck was treated bilaterally to a dose of 50.3 Gy in fractions of 1.48 Gy, and the GTV_{CT} with a margin for subclinical spread and setup inaccuracy was irradiated to a total dose of 68 Gy in 2-Gy fractions. The primary tumor subvolume with the highest density of proliferating cells was defined twice: based on the ^{18}F-FLT PET scan acquired before the initiation of treatment ($GTV_{80\%1}$) and on the scan obtained in the second week ($GTV_{80\%2}$).

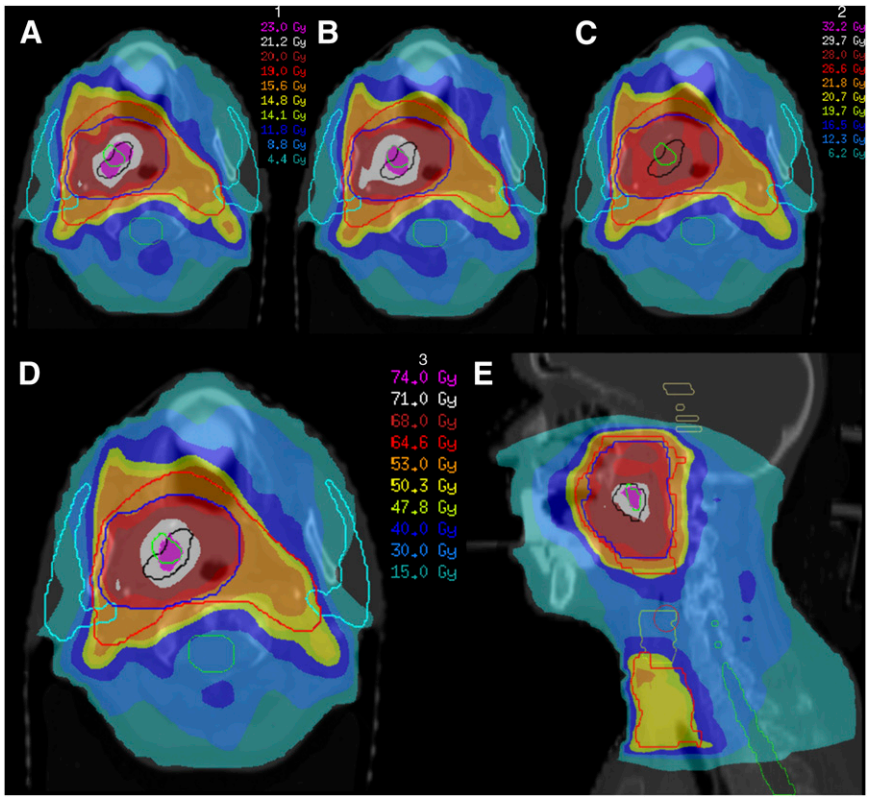

FIGURE 4. Dose escalation to $GTV_{80\%1}$ and $GTV_{80\%2}$ for T3N0M0 oropharyngeal tumor. Using IMRT with integrated simultaneous boost technique, total dose was 50.3 Gy to bilateral cervical lymph node regions (large planning target volume, red) and 68 Gy to primary tumor (small planning target volume, blue). $GTV_{80\%1}$ (black) and $GTV_{80\%2}$ (green) were consecutively irradiated with 2.3 Gy for 10 fractions, resulting in dose of 71 Gy in total and dose of 74 Gy in overlapping region. (A and B) Dose distributions for first 2 wk of treatment (A) and weeks 3 and 4 (B); see legend 1. (C) Dose distribution for remaining 14 fractions without dose escalation; see legend 2. (D and E) Dose distributions of total treatment plan in transverse (D) and sagittal (E) planes; see legend 3. Parotid glands are delineated in sky blue and spinal cord in green.

Subsequently, the $GTV_{80\%1}$ was defined as the boost subvolume for the first 2 wk of treatment, and the $GTV_{80\%2}$ for dose escalation during weeks 3 and 4. From week 5, no increased dose was delivered to a highly proliferative subvolume. The $GTV_{80\%1}$ and $GTV_{80\%2}$ were consecutively irradiated in fractions of 2.3 Gy using the simultaneous integrated boost technique, resulting in a total dose of 74 Gy to the overlapping volume of the $GTV_{80\%1}$ and $GTV_{80\%2}$ and a total dose of 71 Gy to the areas of $GTV_{80\%1}$ and $GTV_{80\%2}$ mismatch. The volume irradiated to a higher dose was small and affected neither the dose to the electively treated volume and primary tumor volume (PTV> and PTV<, respectively) nor the dose to normal tissues (Table 2).

DISCUSSION

Early Response Measurement

Accelerated tumor cell proliferation is an important mechanism of treatment failure in head and neck cancer. A prerequisite for monitoring and early adaptation of treatments that counteract this resistance mechanism is visualization and quantification of the proliferating tumor cell compartment before and during treatment.

^{18}F-FLT is the most widely used PET tracer for imaging tumor proliferation. Alterations in the SUV of ^{18}F-FLT have been used for early response monitoring in a variety of human tumors (*21–24*). Wieder et al. studied rectal cancer patients before treatment, 2 wk after initiation of treatment, and 3–4 wk after completion of treatment (*24*). Although the SUV_{mean} decreased significantly 14 d after the start of chemoradiation, this decrease did not correlate with histopathologic tumor regression. Herrmann et al. assessed 2 groups of patients with non-Hodgkin lymphoma undergoing chemotherapy and found that ^{18}F-FLT SUV_{max} had already decreased significantly after 2 d (*21*). Furthermore, the authors were able to detect a significant difference in reduction of tumoral ^{18}F-FLT uptake between patients reaching a partial response and patients reaching a complete response at the end of therapy. Finally, 2 groups of investigators studied ^{18}F-FLT uptake in breast cancer patients (*22,23*). Kenny et al. examined patients before and 1 wk after neoadjuvant chemotherapy and found that the decrease in ^{18}F-FLT SUV discriminated significantly between patients with clinical response and patients with stable disease (*22*). Pio et al. found that changes in ^{18}F-FLT uptake after 1 course of chemotherapy correlated significantly with changes in tumor size detected by CT (*23*).

Recently, Menda et al. demonstrated in 8 patients with head and neck cancer that initial ^{18}F-FLT uptake and changes early after treatment could be adequately monitored by SUV obtained at 45–60 min (*25*). Furthermore, a study on 15 patients (including 6 with head and neck cancer) provided evidence that changes in ^{18}F-FLT PET SUV_{max} of more than 20%–25% are likely to be therapy-related (*26*). Thus, under the assumption that repetitive quantitative ^{18}F-FLT PET measurements are sufficiently reproducible, ^{18}F-FLT uptake quantified by SUV has the potential to monitor changes in the proliferative activity of tumors early during treatment.

TABLE 2. Comparison of Simultaneous Integrated Boost-IMRT Dose Distributions: Classic Versus ^{18}F-FLT PET–Guided

Parameter	Classic	^{18}F-FLT PET–guided
Organs at risk		
Left parotid gland (Gy)	25.4	25.4
Right parotid gland (Gy)	24.8	24.8
Maximum dose, spinal cord (Gy)	48.2	48.1
PTV>		
Mean dose (Gy)	52.2	52.1
Volume receiving 90% of prescribed dose (%)	99.5	99.5
Volume receiving 95% of prescribed dose (%)	96.7	96.4
PTV<		
Mean dose (Gy)	68.7	69.0
Volume receiving 90% of prescribed dose (%)	99.7	99.6
Volume receiving 95% of prescribed dose (%)	96.9	96.8
PTV≪		
Mean dose, first subvolume (Gy)	NA	73.6
Mean dose, second subvolume (Gy)	NA	74.5
Mean dose, overlap subvolumes (Gy)	NA	74.7

PTV = planning target volume; PTV> = PTV encompassing electively treated volume, i.e., lymph node regions at risk of subclinical metastatic disease; PTV< = PTV encompassing primary tumor; PTV≪ = PTV for dose escalation defined by repetitive ^{18}F-FLT PET (see "Materials and Methods"); NA = not available.

On the basis of these assumptions, our study assessed early response in patients with oropharyngeal tumors treated with radiotherapy or chemoradiation. Overall, there was a significant treatment-induced decrease in ^{18}F-FLT tracer uptake, both in the primary tumor and in cervical lymph node metastases as early as after the fifth fraction of radiotherapy. The reduction in SUVs was more than 2-fold in the initial phase of treatment and a further 2-fold in the fourth week. Clearly, different individual response patterns were also found in this study. Some patients showed a moderate decrease in SUVs, whereas others responded with even an increase in signal intensity. Longer follow-up and a larger patient cohort are necessary to assess whether these individual differences will be discriminative for ultimate tumor response.

One could hypothesize that the concomitant use of chemotherapy may reduce tumor cell proliferation more rapidly than the use of radiotherapy alone. However, the 2 patients treated with chemoradiotherapy in this study did not show a more rapid decrease in ^{18}F-FLT uptake than the others. We will further address this issue in a subsequent study including a larger number of patients treated with chemotherapy. The results of a metaanalysis indicate a survival benefit for concomitant chemotherapy and radiotherapy, and this has become the standard of care for advanced head and neck cancer (*27*). It is therefore important that the effects of chemotherapy on tumor cell proliferation also be investigated in future early-response studies.

Adaptive Radiotherapy Based on ^{18}F-FLT PET/CT

In current practice, radiotherapy planning is based on a single CT scan acquired before the start of treatment. During treatment, however, the tumor and metastatic lymph nodes shrink, and the patient may lose weight. As a result, the dose distribution in the tumor and organs at risk may change. In addition, as demonstrated in this study, biologic aspects of the tumor can change even more rapidly and dramatically. Adaptation of the target volume based on CT or on functional imaging can correct for these treatment-induced alterations. Among other PET radiopharmaceuticals, ^{18}F-FLT is a potential tracer for adaptive radiotherapy because it specifically visualizes one of the tumor characteristics responsible for treatment failure.

In contrast to the early treatment-associated decrease in ^{18}F-FLT uptake, significant changes in GTV_{CT} were detectable only in the fourth week (after 15–18 fractions). Analyses of volumetric changes based on ^{18}F-FLT PET, however, were not successful, possibly because of limitations of the applied PET segmentation techniques. During treatment, the ^{18}F-FLT PET signal intensity within the tumor decreased relative to the background. This observation might argue against the generally accepted phenomenon of accelerated tumor cell repopulation during a course of fractionated radiotherapy. However, the decrease in ^{18}F-FLT PET signal is caused mainly by a rapid reduction of the tumor cell density as a result of the treatment. This does not exclude the possibility that the relative number of proliferating tumor cells, that is, the proliferating fraction, is nevertheless increasing. At the same time, ^{18}F-FLT uptake in the tonsillar region increased most likely because of proliferating inflammatory cells (*28*). These 2 phenomena hampered PET segmentation based on the fixed threshold of 50%. The adaptive threshold delineation based on the signal-to-background ratio performed somewhat better but also failed at the third time point, when ^{18}F-FLT uptake was low. As a consequence, ^{18}F-FLT PET was useful for neither volumetric response monitoring nor adaptation of GTV delineation during treatment. New iterative methods are becoming available, but it is questionable whether these can overcome these limitations (*5,29*). The disturbance by increased proliferative activity in the tonsillar tissue may be a lesser problem in other head and neck subsites.

Dose Escalation to Highly Proliferative Subvolumes

PET may potentially identify parts of the tumor requiring additional radiation doses, for example, areas of high metabolic or proliferative activity or hypoxic subvolumes. In this study, ^{18}F-FLT PET was successfully used to

identify subvolumes with high proliferative activity before and in the second week of therapy in all primary tumors and metastatic lymph nodes. In several patients, the size and location of the subvolumes changed during the initial phase of treatment. Therefore, repetitive imaging for proper monitoring of the highly proliferative subvolumes is necessary. Furthermore, image acquisition late during treatment—for example, the fourth week—does not lead to useful results, because signal intensities are low. Similar findings on temporal changes in hypoxic subvolumes have previously been described, even without any treatment (*30*). Lin et al. studied 7 patients with head and neck cancer undergoing serial ^{18}F-fluoromisonidazole PET scans, separated by 3 d, before the start of treatment. In 4 of these patients, significant dissimilarities in the hypoxic subvolumes were observed within this short time window.

Various theoretic planning studies applying either uniform dose distribution, dose painting, or voxel intensity–based IMRT to ^{18}F-FDG or ^{18}F-fluoromisonidazole PET–avid subvolumes have been published (*8,9,31–34*). Schwartz et al. escalated the total dose up to 75 Gy in a theoretic planning study involving 20 patients with head and neck cancer (*8*). Rajendran et al. demonstrated that using an IMRT technique, the dose to the ^{18}F-fluoromisonidazole PET–detected hypoxic subvolume could be escalated by an additional 10 Gy, and Lee et al. achieved a dose of even 84 Gy in hypoxic areas without exceeding the normal-tissue tolerance (*32,33*). Recently, the clinical feasibility of ^{18}F-FDG PET–based dose escalation using a uniform dose distribution was demonstrated in a phase I clinical trial on patients with head and neck cancer (*6*). With IMRT and a simultaneous integrated boost, the dose was escalated to 72.5 and 77.5 Gy, achieving high local control rates at 1 y of follow-up.

During the initial 4 wk of the current planning study, the radiation dose was escalated to 71 Gy in fractions of 2.3 Gy delivered to the highly proliferative subvolumes $GTV_{80\%1}$ and $GTV_{80\%2}$, resulting in a total dose of 74 Gy in the overlapping volume.

In contrast to ^{18}F-FDG PET, which provides a measure of the total viable tumor cell density, ^{18}F-FLT PET identifies the proliferating cell compartment within the GTV. Although the number of tumor cells is greatly reduced during cytotoxic treatment, cells that survive are triggered to repopulate more effectively during the intervals between treatments, and this process of repopulation is an important cause of treatment failure (*10,11,35,36*). Randomized trials have convincingly shown that accelerated radiotherapy, that is, delivery of the radiation dose in a shorter time, can counteract accelerated repopulation and improve the tumor control probability (*37,38*). Accelerated radiotherapy is now considered the standard for head and neck cancer. Delivering a higher dose to the most actively proliferating parts of the tumor early during the treatment course might have an additive effect and could further reduce the potential of the tumor to recover through accelerated proliferation and repopulation. For elderly patients and patients in less good general condition, dose escalation to the highly proliferative subvolumes might be an alternative to accelerated radiotherapy. Accelerated schedules are accompanied by increased toxicity, in particular early mucosal reactions (*39*). Dose escalation to a relatively small subvolume using IMRT can be accomplished with only limited additional burden to the surrounding normal tissues and thus might be better tolerated by these patients. A clinical study will be initiated to further explore the feasibility and effectiveness of this approach.

CONCLUSION

^{18}F-FLT is a promising PET tracer for imaging tumor cell proliferation in head and neck carcinomas during treatment. This study on oropharyngeal tumors showed that ^{18}F-FLT PET signal changes precede volumetric tumor response assessed by CT or PET and that the tracer is therefore suitable for early response assessment. Furthermore, ^{18}F-FLT PET can define tumor subvolumes with high proliferative activity, and escalation of radiation dose within these regions is technically feasible. At present, adaptive radiotherapy on the basis of ^{18}F-FLT PET volumetric changes is not possible with the commonly available segmentation tools.

ACKNOWLEDGMENTS

We thank the technologists of the Departments of Radiation Oncology and Nuclear Medicine for their assistance and excellent patient care. Prof. Dr. Vincent Grégoire and Dr. John Lee from Université Catholique de Louvain, Belgium, are acknowledged for their kind permission to use the signal-to-background algorithm. This work was supported by EC FP6 funding (Biocare contract LSHC-CT-2004-505785) and by Junior Investigator Grant 2006-38 awarded by the Radboud University Nijmegen Medical Centre, The Netherlands.

REFERENCES

1. Parsons JT, Mendenhall WM, Stringer SP, et al. Squamous cell carcinoma of the oropharynx: surgery, radiation therapy, or both. *Cancer.* 2002;94:2967–2980.
2. Hunt MA, Zelefsky MJ, Wolden S, et al. Treatment planning and delivery of intensity-modulated radiation therapy for primary nasopharynx cancer. *Int J Radiat Oncol Biol Phys.* 2001;49:623–632.
3. Kam MK, Chau RM, Suen J, Choi PH, Teo PM. Intensity-modulated radiotherapy in nasopharyngeal carcinoma: dosimetric advantage over conventional plans and feasibility of dose escalation. *Int J Radiat Oncol Biol Phys.* 2003;56:145–157.
4. Daisne JF, Duprez T, Weynand B, et al. Tumor volume in pharyngolaryngeal squamous cell carcinoma: comparison at CT, MR imaging, and FDG PET and validation with surgical specimen. *Radiology.* 2004;233:93–100.
5. Geets X, Lee JA, Bol A, Lonneux M, Gregoire V. A gradient-based method for segmenting FDG-PET images: methodology and validation. *Eur J Nucl Med Mol Imaging.* 2007;34:1427–1438.
6. Madani I, Duthoy W, Derie C, et al. Positron emission tomography-guided, focal-dose escalation using intensity-modulated radiotherapy for head and neck cancer. *Int J Radiat Oncol Biol Phys.* 2007;68:126–135.
7. Schinagl DA, Vogel WV, Hoffmann AL, van Dalen JA, Oyen WJ, Kaanders JH. Comparison of five segmentation tools for ^{18}F-fluoro-deoxy-glucose-positron

emission tomography-based target volume definition in head and neck cancer. *Int J Radiat Oncol Biol Phys.* 2007;69:1282–1289.
8. Schwartz DL, Ford EC, Rajendran J, et al. FDG-PET/CT-guided intensity modulated head and neck radiotherapy: a pilot investigation. *Head Neck.* 2005; 27:478–487.
9. Vanderstraeten B, Duthoy W, De Gersem W, De Neve W, Thierens H. [^{18}F]fluoro-deoxy-glucose positron emission tomography ([^{18}F]FDG-PET) voxel intensity-based intensity-modulated radiation therapy (IMRT) for head and neck cancer. *Radiother Oncol.* 2006;79:249–258.
10. Maciejewski B, Withers HR, Taylor JM, Hliniak A. Dose fractionation and regeneration in radiotherapy for cancer of the oral cavity and oropharynx: tumor dose-response and repopulation. *Int J Radiat Oncol Biol Phys.* 1989;16:831–843.
11. Withers HR, Taylor JM, Maciejewski B. The hazard of accelerated tumor clonogen repopulation during radiotherapy. *Acta Oncol.* 1988;27:131–146.
12. Rasey JS, Grierson JR, Wiens LW, Kolb PD, Schwartz JL. Validation of FLT uptake as a measure of thymidine kinase-1 activity in A549 carcinoma cells. *J Nucl Med.* 2002;43:1210–1217.
13. Sherley JL, Kelly TJ. Regulation of human thymidine kinase during the cell cycle. *J Biol Chem.* 1988;263:8350–8358.
14. Shields AF, Grierson JR, Dohmen BM, et al. Imaging proliferation in vivo with [F-18]FLT and positron emission tomography. *Nat Med.* 1998;4:1334–1336.
15. Shields AF, Mankoff DA, Link JM, et al. Carbon-11-thymidine and FDG to measure therapy response. *J Nucl Med.* 1998;39:1757–1762.
16. Machulla HJ. Simplified labeling approach for synthesizing 3′-deoxy-3′-^{18}F-fluorothymidine. *J Radioanal Nucl Chem.* 2000;24:843–846.
17. Vogel WV, Wensing BM, van Dalen JA, Krabbe PF, van den Hoogen FJ, Oyen WJ. Optimised PET reconstruction of the head and neck area: improved diagnostic accuracy. *Eur J Nucl Med Mol Imaging.* 2005;32:1276–1282.
18. Daisne JF, Sibomana M, Bol A, Doumont T, Lonneux M, Gregoire V. Tridimensional automatic segmentation of PET volumes based on measured source-to-background ratios: influence of reconstruction algorithms. *Radiother Oncol.* 2003;69:247–250.
19. Dice LR. Measures of the amount of ecologic association between species. *Ecology.* 1945;26:297–302.
20. Bartko JJ. Measurement and reliability: statistical thinking considerations. *Schizophr Bull.* 1991;17:483–489.
21. Herrmann K, Hinrich AW, Buck AK, et al. Early response assessment using 3′-deoxy-3′-[^{18}F]fluorothymidine-positron emission tomography in high-grade non-Hodgkin's lymphoma. *Clin Cancer Res.* 2007;13:3552–3558.
22. Kenny L, Coombes RC, Vigushin DM, Al-Nahhas A, Shousha S, Aboagye EO. Imaging early changes in proliferation at 1 week post chemotherapy: a pilot study in breast cancer patients with 3′-deoxy-3′-[^{18}F]fluorothymidine positron emission tomography. *Eur J Nucl Med Mol Imaging.* 2007;34:1339–1347.
23. Pio BS, Park CK, Pietras R, et al. Usefulness of 3′-[F-18]fluoro-3′-deoxythymidine with positron emission tomography in predicting breast cancer response to therapy. *Mol Imaging Biol.* 2006;8:36–42.
24. Wieder HA, Geinitz H, Rosenberg R, et al. PET imaging with [^{18}F]3′-deoxy-3′-fluorothymidine for prediction of response to neoadjuvant treatment in patients with rectal cancer. *Eur J Nucl Med Mol Imaging.* 2007;34:878–883.
25. Menda Y, Boles Ponto LL, Dornfeld KJ, et al. Kinetic analysis of 3′-deoxy-3′-^{18}F-fluorothymidine (^{18}F-FLT) in head and neck cancer patients before and early after initiation of chemoradiation therapy. *J Nucl Med.* 2009;50:1028–1035.
26. de Langen AJ, Klabbers B, Lubberink M, et al. Reproducibility of quantitative ^{18}F-3′-deoxy-3′-fluorothymidine measurements using positron emission tomography. *Eur J Nucl Med Mol Imaging.* 2009;36:389–395.
27. Pignon JP, le Maitre A, Maillard E, Bourhis J. Meta-analysis of chemotherapy in head and neck cancer (MACH-NC): an update on 93 randomised trials and 17,346 patients. *Radiother Oncol.* 2009;92:4–14.
28. Troost EG, Vogel WV, Merkx MA, et al. ^{18}F-FLT PET does not discriminate between reactive and metastatic lymph nodes in primary head and neck cancer patients. *J Nucl Med.* 2007;48:726–735.
29. van Dalen JA, Hoffmann AL, Dicken V, et al. A novel iterative method for lesion delineation and volumetric quantification with FDG PET. *Nucl Med Commun.* 2007;28:485–493.
30. Lin Z, Mechalakos J, Nehmeh S, et al. The influence of changes in tumor hypoxia on dose-painting treatment plans based on ^{18}F-FMISO positron emission tomography. *Int J Radiat Oncol Biol Phys.* 2008;70:1219–1228.
31. Grosu AL, Souvatzoglou M, Roper B, et al. Hypoxia imaging with FAZA-PET and theoretical considerations with regard to dose painting for individualization of radiotherapy in patients with head and neck cancer. *Int J Radiat Oncol Biol Phys.* 2007;69:541–551.
32. Lee NY, Mechalakos JG, Nehmeh S, et al. Fluorine-18-labeled fluoromisonidazole positron emission and computed tomography-guided intensity-modulated radiotherapy for head and neck cancer: a feasibility study. *Int J Radiat Oncol Biol Phys.* 2008;70:2–13.
33. Rajendran JG, Schwartz DL, O'Sullivan J, et al. Tumor hypoxia imaging with [F-18] fluoromisonidazole positron emission tomography in head and neck cancer. *Clin Cancer Res.* 2006;12:5435–5441.
34. Thorwarth D, Eschmann SM, Scheiderbauer J, Paulsen F, Alber M. Kinetic analysis of dynamic ^{18}F-fluoromisonidazole PET correlates with radiation treatment outcome in head-and-neck cancer. *BMC Cancer.* 2005;5:152.
35. Kim JJ, Tannock IF. Repopulation of cancer cells during therapy: an important cause of treatment failure. *Nat Rev Cancer.* 2005;5:516–525.
36. Petersen C, Zips D, Krause M, et al. Repopulation of FaDu human squamous cell carcinoma during fractionated radiotherapy correlates with reoxygenation. *Int J Radiat Oncol Biol Phys.* 2001;51:483–493.
37. Bourhis J, Overgaard J, Audry H, et al. Hyperfractionated or accelerated radiotherapy in head and neck cancer: a meta-analysis. *Lancet.* 2006;368:843–854.
38. Overgaard J, Hansen HS, Specht L, et al. Five compared with six fractions per week of conventional radiotherapy of squamous-cell carcinoma of head and neck: DAHANCA 6 and 7 randomised controlled trial. *Lancet.* 2003;362:933–940.
39. Kaanders JH, Pop LA, Marres HA, et al. ARCON: experience in 215 patients with advanced head-and-neck cancer. *Int J Radiat Oncol Biol Phys.* 2002;52: 769–778.